Vector meson production and inclusive $K^0_s K^0_s$ final state at HERA

M. Barbi [a]
(on behalf of the H1 and ZEUS Collaborations)

[a]McGill University, Physics Department
Montreal, Quebec
Canada

Measurements of vector mesons at HERA allow a detailed study of diffractive and non-diffractive production mechanisms, fragmentation and decay branching ratios. Results are presented on hadronic resonance measurements. In addition, the first observation of two meson states at masses around 1500 MeV and 1700 MeV are reported using inclusive $K^0_s K^0_s$ production in deep inelastic *ep* scattering in ZEUS at HERA.

1. Vector Meson Production at HERA

Production of light and heavy vector mesons (V) in exclusive and in proton dissociation processes has been studied in *ep* reactions at HERA in a wide range of the γp centre-of-mass energy W and photon virtuality Q^2. For very low Q^2 and $W > 10$ GeV, these reactions display features characteristic of a soft diffractive process. The cross sections rises weakly with the energy W, $\sigma_V(W) \propto W^\delta$ ($\delta \simeq 0.22$), and has a steep exponential t dependence, where t is the squared four-momentum transfer at the proton vertex. Such processes are well described within the framework of Regge phenomenology [1,2,3] and the Vector-Meson Dominance model (VDM) [4,5], where the photon is assumed to fluctuate into a vector meson before scattering from the proton via Pomeron exchange. However, this approach fails at high values of Q^2 or high vector meson masses. In the hard regime, models based on perturbative QCD (pQCD) [6,7] can be used to describe the vector meson production. The photon fluctuates into a $q\bar{q}$ state and the quark dipole interacts with the proton in the lowest order via two gluons exchange [8,9,10,11]. The exchange of the gluon ladder has also been calculated in the leading logarithm approximation (LLA) [8,11,12,13]. The cross section is related to the rise of the gluon density in the proton as x decreases, where x is the Bjorken scale variable, and has a strong W dependence, $\sigma_V(W) \propto W^\delta$ ($\delta \simeq 0.8$.)

In this contribution, perturbative QCD models are compared with results from vector meson production in photoproduction and deep inelastic scattering at HERA.

1.1. Exclusive Vector Meson Production

Figure 1 shows $\sigma_{tot}^{\gamma^* p \to J/\psi p}$ from ZEUS [14,15] and H1 [16] as a function of W for fixed Q^2, and also in photoproduction. The data is fitted with W^δ. The ZEUS measurements are shown in table 1. The results are compatible with results in photoproduction from H1 [17] $\delta = 0.83 \pm 0.07(stat \oplus syst)$ and ZEUS [18] $\delta = 0.69 \pm 0.02(stat) \pm 0.03(syst)$. The cross sections are also compared to pQCD predictions from Frankfurt, Koepf and Strikman (FKS) [19] using CTEQ4M PDF [20], and from Martin, Ryskin and Teubner (MRT) [21] using CTEQ5M PDF [22]. The results are sensitive to the PDF used and have large theoretical uncertainties, but they qualitatively describe the strong W-dependence of the cross section. They also indicate that at high vector meson masses M_V, a hard regime already exist at very low values of Q^2, and that M_V^2 may set a hard scale.

The Q^2-dependence of the δ parameter is shown in Fig. 2 for the light vector meson ρ^0 from ZEUS [23] and H1 [24], and for J/ψ in photoproduction from H1 [17]. At very low values of Q^2, Regge phenomenology and VDM models describe

Table 1
Results from the fit of W^δ to $\sigma_{tot}^{\gamma^* p \to J/\psi p}$ measured by ZEUS at different values of Q^2 .

Q^2 (GeV^2)	0.4	3.2	6.8	16
δ	$0.84 \pm 0.38^{+0.10}_{-0.04}$	$0.33 \pm 0.22^{+0.37}_{-0.46}$	$0.84 \pm 0.24^{+0.31}_{-0.43}$	$0.37 \pm 0.25^{+0.30}_{-0.22}$

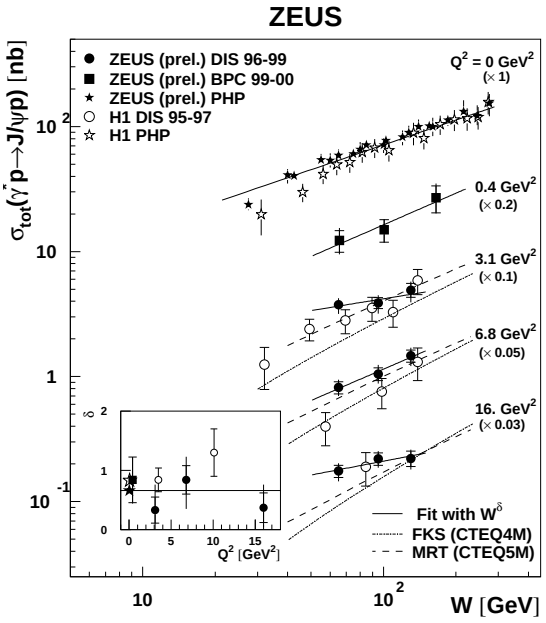

Figure 1. W-dependence of J/ψ electroproduction at different values of Q^2, and comparison with predictions from FKS and MRT models. The inset displays the fitted value of δ as a function of Q^2.

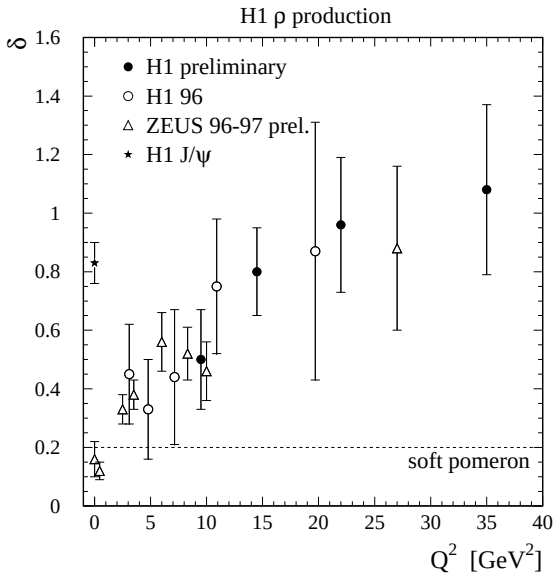

Figure 2. Results from the fit using $\sigma_V(W) \propto W^\delta$ for the light and heavy vector mesons ρ^0 and J/ψ, respectively. At low values of Q^2, soft processes are dominant for ρ^0 production, while hard processes dominate for J/ψ production already at $Q^2 = 0$.

the ρ^0 meson production. However, the energy W-dependence becomes steeper at high Q^2, with a smooth transition from soft to hard regime. On the other hand, the J/ψ cross section has a strong energy dependence already at $Q^2 = 0$. These results indicate that Q^2 may also set a hard scale.

1.2. Vector Meson Production with Proton Dissociation

It was predicted [25,26] that hard processes may occur at high $-t$. Typical elastic vector meson production has $-t < 1$ GeV^2, and cannot be used to verify these predictions. On the other hand, proton-dissociation processes have higher values of $-t$. Figure 3 shows the differential cross sections of ρ, ϕ and J/ψ vector mesons in the photoproduction proton-dissociative reaction $\gamma p \to VY$ in the range $80 < W < 120$ GeV and $x > 0.01$ from ZEUS [27], where Y is the dissociated hadronic system. The data is compared to predictions from Forshaw and Poludniowski [11] using LLA BFKL [28,29]. The results are in good

agreement, indicating that pQCD can describe vector meson production at high $-t$ regime.

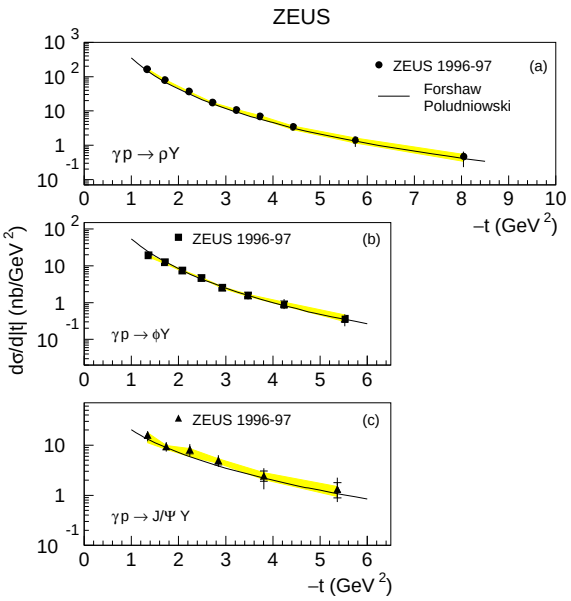

Figure 3. The differential cross sections $\mathrm{d}\sigma_{\gamma p\to VY}/\mathrm{d}|t|$ for: (a) ρ^0, (b) ϕ, and (c) J/ψ photoproduction. The solid lines show the predictions from Forshaw and Poludniowski using LLA BFKL. The inner bars indicate the statistical uncertainty and the outer bars represent the statistical and systematic uncertainties added in quadrature. The shaded bands represents the uncertainties due to the modelling of the hadronic-system Y.

1.3. Summary

The results presented in this contribution indicates a smooth transition from soft to hard regime. They also show that pQCD describes the vector production in the hard regime, and that Q^2, M_V^2 and $-t$ can set a hard scale.

2. Inclusive $K_s^0K_s^0$ Final State in Deep Inelastic Scattering at HERA

The $K_s^0K_s^0$ system is expected to couple to scalar and tensor glueballs. This has motivated intense experimental and theoretical study during the past few years [30,31]. Lattice QCD calculations [32,33] predict the existence of a scalar glueball with a mass of 1730 ± 100 MeV and a tensor glueball at 2400 ± 120 MeV. The scalar glueball can mix with $q\overline{q}$ states with $I = 0$ from the scalar meson nonet, leading to three $J^{PC} = 0^{++}$ states whereas only two can fit into the nonet. Experimentally, four states with $J^{PC} = 0^{++}$ and $I = 0$ have been established [34]: $f_0(980)$, $f_0(1370)$, $f_0(1500)$ and $f_0(1710)$.

The state most frequently considered to be a glueball candidate is $f_0(1710)$ [34] , but its gluon content has not yet been established. This state was first observed in radiative J/ψ decays [35] and its angular momentum $J = 0$ was established by the WA102 experiment using a partial-wave analysis in the K^+K^- and $K_s^0K_s^0$ final states[36] . Observation of $f_0(1710)$ in $\gamma\gamma$ collisions may indicate a large quark content. A recent publication from L3 [37] reports the observation of two states in $\gamma\gamma$ collisions above 1500 MeV, the well-established $f_2'(1525)$ [34] and a broad resonance at 1760 MeV. It is not clear if the latter state is the $f_0(1710)$.

The ep collisions at HERA provide an opportunity to study resonance production in a new environment. Production of K_s^0 particles has been studied previously at HERA [38,39,40]. In this contribution, the first observation of resonances in the $K_s^0K_s^0$ final state in inclusive deep inelastic ep scattering (DIS) is reported [41].

2.1. Results

The data used for this study correspond to a total integrated luminosity of 120 pb^{-1} collected in ZEUS during the 1996-2000 running period.

Oppositely charged track pairs reconstructed by the ZEUS central tracking detector (CTD) and assigned to a secondary vertex were selected and combined to form K_s^0 candidates. Both tracks were assigned the mass of a charged pion and the invariant-mass $M(\pi^+\pi^-)$ was calculated. Only

events with at least one pair of K_s^0 candidates were selected. The invariant mass of the K_s^0 pair candidate $M(K_s^0, K_s^0)$ was reconstructed in the range $0.995 < M(K_s^0 K_s^0) < 2.795$ GeV.

Figure 4 shows the distribution in x and Q^2 of selected events containing at least one pair of K_s^0 candidates. The virtual photon-proton center of mass energy is in the range $50 < W < 250$ GeV.

Figure 5 shows the $M(\pi^+\pi^-)$ distribution in the range $0.45 < M(\pi^+\pi^-) < 0.55$ GeV after the K_s^0 pair candidate selection.

A cut $cos\theta_{K_s^0 K_s^0} < 0.92$ is applied to the selected K_s^0 pair candidates, where $\theta_{K_s^0 K_s^0}$ is the opening angle between the two K_s^0 candidates in the laboratory frame. This cut removes phase-space effects and the presence of $f_0(980)/a_0(980)$ at the threshold, which decays to collinear K_s^0 pairs affecting the measurement in the 1300 MeV mass region.

Figure 6 shows the $K_s^0 K_s^0$ invariant-mass spectrum in the range $0.995 < M_{K_s^0 K_s^0} < 2.795$ GeV for data with $cos\theta_{K_s^0 K_s^0} < 0.92$ (filled circles with error bar). Two clear peaks are seen, one around 1500 MeV, consistent with the well-established $f_2'(1525)$ [34], and the other around 1700 MeV, close to $f_0(1710)$ [34]. There is also an enhancement around 1300 MeV, consistent with the $f_2(1270)/a_2(1320)$ interference.

It was found that most of the K_s^0 pair candidates selected after all cuts are in the "gluon-rich" region $x_p = 2p_B/Q > 1$ of the target region of the Breit frame, which corresponds to the remnant of the proton [42,43] , where p_B is the absolute momentum of the $K_s^0 K_s^0$ in the Breit frame.

2.2. Summary

The first observation in deep inelastic ep scattering of a state near 1525 MeV, consistent with $f_2'(1525)$, and another close to $f_0(1710)$ is reported.

An enhancement which can be interpreted as the $f_2(1270)/a_2^0(1320)$ interference is observed, but its measurement is affected by the presence of the $f_0(980)/a_0(980)$ at the $K_s^0 K_s^0$ threshold.

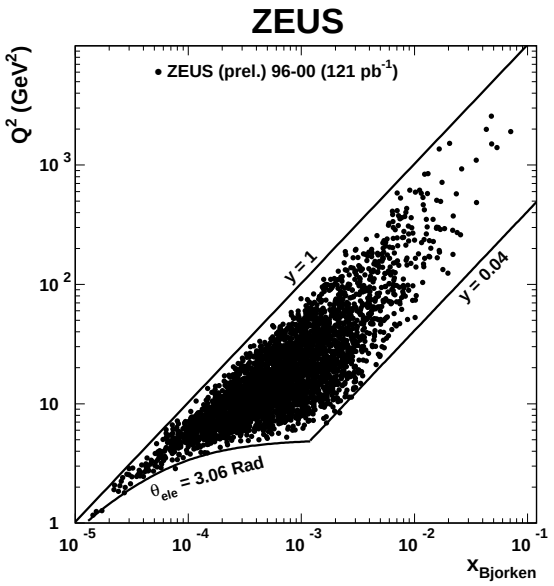

Figure 4. The distribution in x and Q^2 of events passing all selection cuts. The $y = 0.04$ and $\theta_{ele} = 3.1$ rad lines delineate approximately the kinematic region selected, where y is the fractional energy transferred to the hadronic final state and θ_{ele} is the polar angle of the scattered electron in the ep reaction. The $y = 1$ line indicates the kinematic limit for HERA running with 920 GeV proton.

REFERENCES

1. A. Donnachie and P.V. Landshoff, Phys. Lett. B 470 (1999) 243.
2. A. Donnachie and P.V. Landshoff, Phys. Lett. B 478 (2000) 146.
3. E. Martynov, E. Predazzi and A. Prokudin, Preprint hep-ph/0112242 (2001).
4. J.J. Sakurai, Ann. Phys. 11 (1960) 1.
5. J.J. Sakurai, Phys. Rev. Lett. 22 (1969) 981.
6. M.G. Ryskin, Z. Phys. C 57 (1993) 89.
7. S.J. Brodsky et al., Phys. Rev. D 50 (1994) 3134.
8. J.R. Forshaw and M.G. Ryskin, Z. Phys. C 68 (1995) 137.

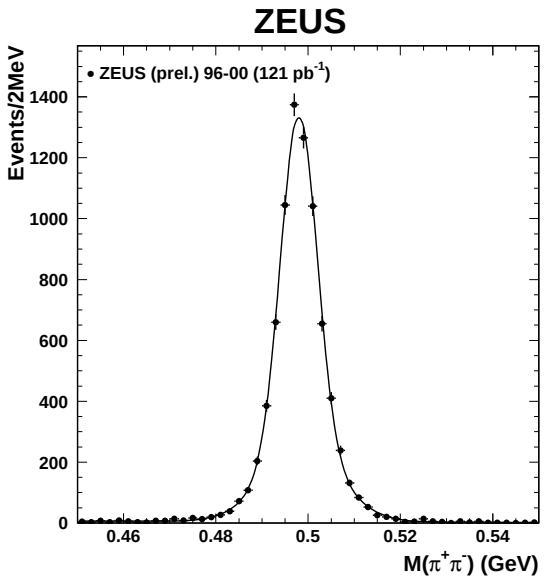

Figure 5. The distribution of $\pi^+\pi^-$ invariant-mass events with two K_s^0 candidates passing all selection cuts, The solid line shows the result of a fit using one linear and two Gaussian functions.

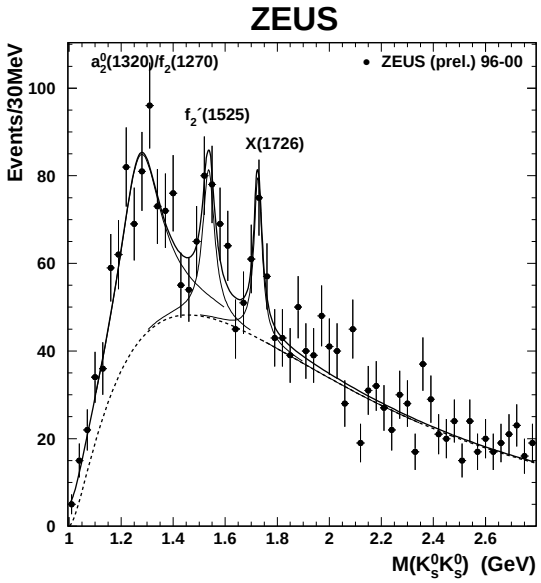

Figure 6. The $K_s^0 K_s^0$ invariant-mass spectrum. The solid line is the result of a fit using three Breit-Wigner and a background function.

9. I.F. Ginzburg and D.Yu. Ivanov, Phys. Rev. D 54 (1996) 5523.
10. D.Yu. Ivanov et al., Phys. Lett. B 478 (2000) 101.
11. J.R Forshaw and G. Poludniowski, Preprint hep-ph/0107068 (2001).
12. D.Yu. Ivanov, Phys. Rev. D 53 (1996) 3564.
13. J. Bartels et al., Phys. Lett. B 375 (1996) 301.
14. ZEUS Coll., J. Breitweg et al., Eur. Phys. J. C 6 (1999) 603.
15. ZEUS Coll., Contrib. pap. 559 to the Eur. Phys. Soc. Conference, Budapest 2001.
16. H1 Coll., C. Adloff et al., Eur. Phys. J. C 10 (1999) 373.
17. H1 Coll., C. Adloff et al., Phys. Lett. B 483 (2000) 23.
18. ZEUS Coll., Eur. Phys. J. C 24 (2002) 345.
19. L. Frankfurt, W. Koepf and M. Strikman, Phys. Rev. D 57 (1998) 512.
20. H.L. Lai et al., Phys. Rev. D 55 (1997) 1280.
21. A.D. Martin, M.G. Ryskin and T. Teubner, Phys. Rev. D 26 (1999) 14022.
22. CTEQ Coll., H.L. Lai et al., Eur. Phys. J. C 12 (2000) 375.
23. ZEUS Coll., Contrib. pap. 594 to the Eur. Phys. Soc. Conference, Budapest 2001.
24. H1 Coll., Contrib. pap. 989 to the 31st Internat. Conference on High Ene. Phys., Amsterdam, 2002.
25. L. Frankfurt and M. Strikman, Phys. Rev. Lett. 63 (1989) 1914.
26. A.H. Mueller and W.K. Tang, Phys. Lett. B 284 (1992) 123.
27. ZEUS Coll., S. Chekanov et al., Eur. Phys. J. C 26 (2003) 389.
28. E.A. Kuraev, L.N. Lipatov and V.S. Fadin, Sov. Phys. JETP 45 (1977) 199.
29. Ya.Ya. Balitskiĭ and L.N. Lipatov, Sov. J. Nucl. Phys. 28 (1978) 822.
30. S. Godfrey, J. Napolitano, Rev. of Modern Phys. 71 (1999) 1411.

31. E. Klempt, Preprint hep-ex/0101031 (2000).
32. C.J. Morningstar, M. Peardon, Phys. Rev. D 60 (1999) 034509.
33. C. Michel and M. Teper, Nucl. Phys. B 314 (199) 347.
34. K. Hagiwara et al., Phys. Rev. D 66 (2002) 1.
35. BES Coll., J. Z. Bai et al., Phys. Rev. Lett. 77 (1996) 3959.
36. WA102 Coll., D. Barberis et al., Phys. Lett. B 453 (1999) 305.
37. L3 Coll., M. Acciari et al., Phys. Lett. B 501 (2001) 173.
38. ZEUS Coll., J. Breitweg et al., Eur. Phys. J. C 2 (1998) 77.
39. ZEUS Coll., M. Derrick et al., Z. Phys. C 68 (1995) 29.
40. H1 Coll., S. Aid et al., Nucl. Phys. B 480 (1996) 3.
41. S. Paganis, for the H1 and ZEUS Coll., Preprint hep-ex/0305056 (2003).
42. R.P. Feynman, Photon-Hadron Interactions (1972).
43. K.H. Streng, T.F. Walsh and P.M. Zerwas, Z. Phys. C 2 (1979) 237.